Magnetotransport in transparent single-wall carbon nanotube networks

Manu Jaiswal,[1,*] Wei Wang,[2] K. A. Shiral Fernando,[2] Ya-Ping Sun,[2] and Reghu Menon[1]
[1]*Department of Physics, Indian Institute of Science, Bangalore 560012, India*
[2]*Department of Chemistry and Laboratory for Emerging Materials and Technology, Clemson University, Clemson, South Carolina 29634-0973, USA*

(Received 17 February 2007; revised manuscript received 19 May 2007; published 6 September 2007)

An experimental study of the low temperature magnetotransport in optically transparent single-wall carbon nanotube (SWNT) networks is reported. The SWNT network shows Coulomb gap variable-range hopping conduction at low temperatures. The magnetoresistance (MR) involves the interplay of two phenomena: a forward interference process leading to negative MR together with shrinkage of electronic wave function contributing to the positive MR. These two mechanisms fit the low-field data. The analysis of magnetotransport data gives an estimate for intrinsic parameters including localization length and Coulomb gap. The temperature dependence of the forward interference mechanism is shown to follow an inverse power-law dependence with an exponent close to 1, indicating the weak scattering process involved in the transport.

DOI: 10.1103/PhysRevB.76.113401 PACS number(s): 73.63.Fg, 73.43.Qt

The electronic properties of single-wall carbon nanotube (SWNT) systems have attracted considerable interest due to their ideal one-dimensional structure and the possibilities for a wide range of disorder. A significant variation in the transport properties, from diffusive to ballistic, has been reported, and this has led to an ambiguous scenario. Since it is well known that one-dimensional systems are highly susceptible to disorder-induced localization and Coulomb interactions, low temperature magnetotransport measurements can give insight into this subtle interplay. The magnetotransport has been investigated in graphite nanotubules,[1] macroscopic bundles of intercalated multiwall carbon nanotubes (MWNTs),[2] strongly disordered MWNTs,[3] entangled SWNT mats,[4] macroscopic doped SWNTs,[5] and disordered individual SWNTs.[6] Especially in the case of SWNT, minute variations in structural disorder can lead from weak to strong localization, and this yields complex and intriguing features in the analysis of magnetotransport data. Further, there is lack of detailed understanding of the physics in the latter regime unlike in the case of the interference process in the weak localization regime near the metal-insulator (M-I) transition.

In this Brief Report, we report the magnetotransport measurements on a transparent network of SWNTs. As already reviewed by Grüner and co-workers[7,8] and Zhang *et al.*,[9] these networks have important applications as flexible transparent electrodes in organic optoelectronics. Our networks show 85% transparency at 550 nm wavelength, which is comparable to that of indium tin oxide transparent electrodes. The SWNTs were prepared by carbon-arc method resulting in a mixture of metallic and semiconducting nanotubes of which the latter are two-thirds. The semiconducting nanotubes were separated from the metallic ones by means of separating agents that preferentially associate with the former. This yields about 90% enriched semiconducting SWNTs, and the process is described in detail elsewhere.[10,11] In the preparation of the transparent nanotube film, 5 mg semiconducting SWNTs was dispersed in 50 ml dimethylformamide (DMF) via homogenization for 30 min, followed by sonication for 60 min. Then, 15 ml of the dispersion solution was sprayed onto a heated clean glass slide on a hot plate at 150 °C. A typical scanning electron microscope (SEM) image of the network is shown in Fig. 1. SWNTs were randomly laid on the glass surface to form an interconnected nanotube network. The nanotubes have a typical bundle diameter of 10–20 nm and an average length of well beyond 1 μm.

The magnetotransport experiments were performed with a standard four-probe dc method in a Janis variable-temperature cryogenic system equipped with an 11 T superconducting magnet. The magnetic field was applied both perpendicular and parallel to the network plane. The current used in low temperature transport measurements are below 0.5 μA, and the heat dissipation is typically less than 30 nW. The temperature was stable to within 20 mK during the field sweep.

The temperature dependence of resistance of the network is shown in Fig. 2(a). The resistance ratio is $R_{4.2\ \mathrm{K}}/R_{300\ \mathrm{K}} \sim 57$, and it increases significantly for $T < 20$ K, suggesting a "hopping-type" conduction mechanism. Recently, Skákalová *et al.* have reported current-voltage (I-V) characteristics and temperature dependence of conductance on transparent SWNT networks and found that the transport is consistent with hopping conduction with important contribution from the disordered metallic tubes.[12] To understand the exact nature of charge transport in such systems, our data are ana-

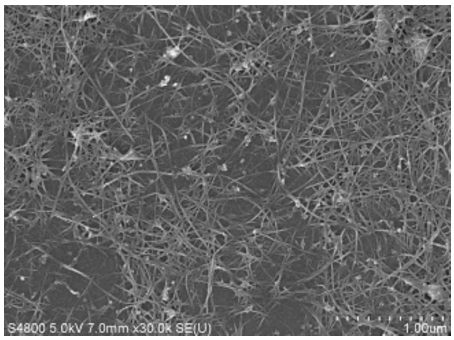

FIG. 1. SEM image of the transparent SWNT network (the scale bar is 1 μm).

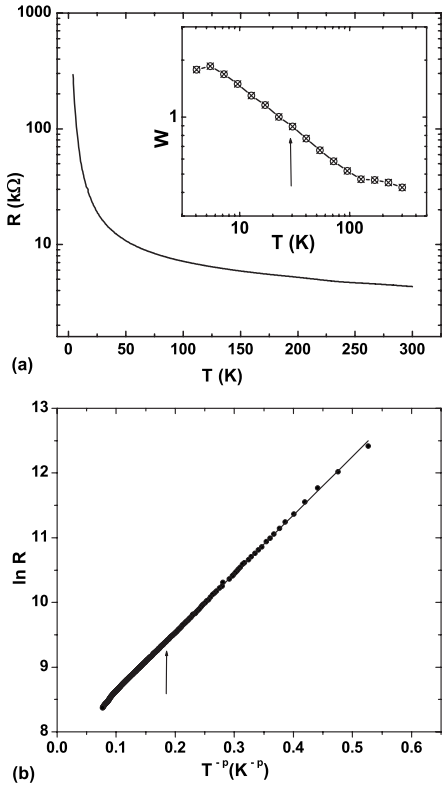

FIG. 2. (a) Temperature dependence of the zero-field resistance. Inset: Reduced activation energy W vs T. (b) $\ln R$ vs T^{-p} plot showing the linear relationship (arrows indicate limit of linear regime fit).

lyzed using the resistivity curve derivative analysis method.[13] The reduced activation energy (W) is estimated as $W(T)=-\partial \ln R(T)/\partial \ln T$. The W plot [inset of Fig. 2(a)] yields a negative slope indicating that the network is in the insulating regime at low temperatures, with an exponential temperature dependence (exponent $p=0.45-0.5$), as described below. In Fig. 2(b), the logarithmic resistance is plotted indicating the linear relationship with the appropriate power of temperature. The exponent $p=\frac{1}{2}$ can arise from various transport regimes such as Mott variable-range hopping (VRH) in one dimension and Coulomb Gap (CG) VRH.[13] One-dimensional Mott VRH is an unlikely scenario in this case as the value obtained for the obtained localization length ($\sim 0.2\ \mu$m) would be physically unrealistic for the disordered system, as earlier noted by Vavro *et al.*[5] The CG-type transport is also consistent with the same exponent but involves the formation of an energy gap at the Fermi level on account of Coulomb interactions. Near the Fermi level, the density of states (DOS) follows a power-law dependence, $N(E)=N_0|E-E_F|^{\gamma}$ with $\gamma=1$ for two dimensions and $\gamma=2$ for three dimensions.[13] The Coulomb correlations in this transparent network are much more significant due to the unscreened nature of interactions with respect to the bulk SWNTs.[14] Usually, this is a low temperature effect since at higher temperatures, the thermal energy is greater than the size of the gap. The CG VRH has also been reported recently on an isolated single tube of SWNTs with some disorder[6] and previously on SWNT-polymer composites with low volume packing fraction of tubes.[15] Alternatively, the same energy gap can also arise from charging energy effect when the network is considered as a granular metal. In this case, the tunnel junction across the tubes comprises a parallel plate capacitor and a resistor, with tunneling taking place across the metallic grains. The value of the Coulomb gap is useful to distinguish these mechanisms. The temperature dependence of resistance for CG VRH is universal for both two-dimensional and three-dimensional (3D) disordered electronic systems and is given by

$$R(T) = R_0 \exp[(T_0/T)^{1/2}], \tag{1}$$

where $T_0=\beta e^2/k_B\kappa\lambda$, κ is the dielectric constant, λ is the localization length, and the numerical coefficient β has the value 6.2 in two dimensions and 2.8 in three dimensions. The values of R_0 and T_0 are 2.275 kΩ and 128 K, respectively. The value of characteristic "Coulomb gap" temperature T_{CG} can be estimated as $T_0/T_{CG}=\beta(4\pi)^{1/2}$; $T_{CG}=12.9$ K. Since the linear regime extends to a higher temperature ($\sim$30 K) as seen from the W plot, the possibility of correlations between grains contributing to the transport should be considered, as discussed below.

The magnetoresistance (MR) data in the CG-VRH regime are shown in Figs. 3(a) and 3(b) as a function of transverse field at low temperatures. At low fields, the MR is negative and linear with magnetic field [Fig. 3(b)] for $T \geqslant 4.2$ K. At high field, the MR decreases and even the sign changes to positive at lower temperatures, being entirely positive at 1.3 K [Fig. 3(a)]. Conventionally, this type of negative MR is attributed to the suppression of quantum localization corrections to the Drude conductivity in systems near the M-I transition.[16] However, this interpretation of the negative MR is not plausible in disordered SWNT since the temperature dependence of resistance is in the CG-VRH regime. Hence, alternate explanations based on the strongly localized nature of the system should be considered. This negative MR in strong localization regime is attributed to forward interference effects of electrons undergoing tunneling hops.[17–19] In the model by Nguyen *et al.*,[17] the MR was shown to be linear with field, originating from multisite hops that interfere destructively in the absence of the field. An identical result was also obtained by Raikh and Wessels by taking into account the forward interference process between sites with scattering process involving a third, randomly distributed site.[18] Schirmacher also arrived at a similar result by considering an "interference hole" or a region with no destructive interference in the three-site hopping process.[19] In this complex scenario, the choice of the exact model would depend on the nature of disorder (both intra- and intertube) and scattering process in the system.

In addition to the above mentioned negative MR, the positive MR observed at lower temperatures and high magnetic fields can be attributed to the wave-function shrinkage process.[6] The increased resistance results from a decrease in the probability of hopping on account of the contraction of the wave function's exponential tails in the presence of the field. For CG-VRH transport, the low-field ($\eta \gg \lambda$) positive MR is governed by the equation[20]

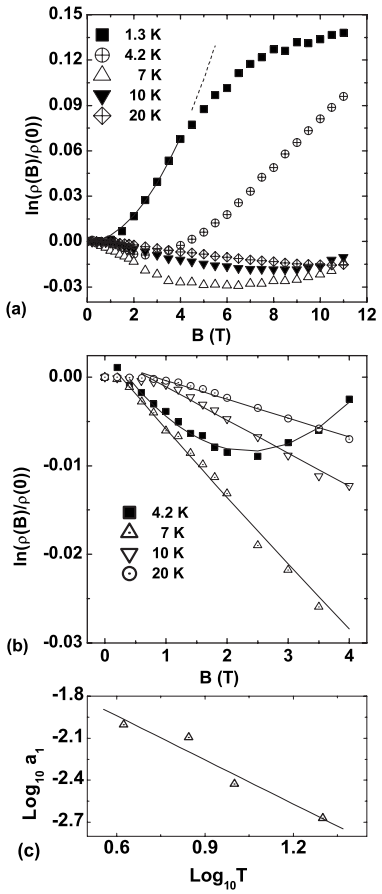

FIG. 3. (a) Transverse field dependence of MR at various temperatures. The solid line is the wave-function shrinkage fit to low-field ($B<4$ T) positive MR at 1.3 K. (b) Low-field MR at various temperatures. The solid lines are fits to Eq. (3) described in text. (c) Coefficient of term linear in field (a_1) vs T.

$$\ln[\rho(B)/\rho(0)] = 0.0015(\lambda/\eta)^4(T_0/T)^{3/2}, \tag{2}$$

where $\eta=\sqrt{\hbar/eB}$ is the magnetic length. The MR at 1.3 K is positive even at the lowest fields and a fit to Eq. (2) [see Fig. 3(a)] gives the value of localization length $\lambda=6$ nm. This value is comparable to the results obtained on disordered individual SWNTs, where the reported localization lengths are 4.5 and 15 nm for as-deposited and annealed tubes, respectively.[6] Substituting λ in Eq. (1), the obtained dielectric constant κ for our network of randomly oriented tubes is 61, which is intermediate between the values for graphite ($\kappa=12$) and annealed SWNT with disorder measured along the tube axis ($\kappa=80$).[6] The Coulomb gap[20] can be estimated as $\Delta_{CG}=e^3N(E_F)^{1/2}/\kappa^{3/2}=1.1$ meV, where the dielectric constant is given by $\kappa=[4\pi\varepsilon_0+4\pi e^2N(E_F)\lambda^2]$ and $N(E_F)$ is the unperturbed DOS at the Fermi level.[21] The value of characteristic Coulomb gap temperature T_{CG} obtained from the gap is $T_{CG}=\Delta_{CG}/k_B=12.8$ K, in good agreement with the value obtained from resistance data. The charging energy $E_c=e^2/2C$ can be estimated from the geometrical capacitances of the network of bundles.[15] The estimate of Δ_{CG} is in excellent agreement with the value for Coulomb charging energy (1.3 ± 0.3 meV), indicating that charging energy plays a dominant role in the gap formation. This soft gap is occurring in metallic tubes ($\sim$10% of tubes), which play an important role in the low temperature transport.[5,12] It should be noted, however, that such a comparison is based on the assumption that the fluctuations in grain work function are larger than E_c. It then follows that at low temperature, the grains will be charged and correlation between the charges of different grains will give rise to a Coulomb gap.[20] The value of DOS for the network obtained from this analysis is 0.09 eV^{-1} nm^{-3}, which correlates with that for metallic tubes upon scaling with the typical estimates of volume packing fraction of tubes (20%–25%) for transparent networks.[15] A correlation of the localization length with the size of SWNT bundles in the network has been suggested by Benoit *et al.*,[15] and this compares well for our system (10–20 nm bundle diameters). Incidentally, this length scale is also of the same order of magnitude as the disorder along the tube length of an individual SWNT;[22] however, that system shows distinctly different transport properties in comparison to our network. The values of λ and Δ_{CG} obtained from this analysis are quite significant to get an insight into the extent of disorder in SWNTs. However, a precise definition for localization length is a subject of debate for nanotube systems and these parameters are rather indicative values.[5] At high fields, at 1.3 K, the positive MR saturates [Fig. 3(a)], as expected from the VRH theory.[5,20]

For the experimental data at 4.2 K and higher temperatures, the MR involves contributions from the forward interference mechanism,[17–19] as well as from wave-function shrinkage. As previously shown,[23–25] these contributions are additive and the total MR is given by

$$\ln[(\rho(B)/\rho(0)\ ] = -a_1B + a_2B^2 + a_3, \tag{3}$$

where a_1 is the coefficient in forward interference mechanism, a_2 is the coefficient of the wave-function shrinkage term, and a_3 accounts for the complex nature of hops at very low fields.[18] A fit to the experimental data for low and intermediate fields ($B<4$ T) is carried out with the above equation, as shown in Fig. 3(b). It is necessary to include the term a_3 in order to obtain proper fits to low-field data but the fits are not extended to 0 T. Moreover, Raikh and Wessels have shown that the energy dependence of electron scattering and absorption or emission of phonon at the scatterer are two relevant processes at very low fields.[18] These effects can produce an initial quadratic field dependence that changes over to the linear one. Our data are suggestive of this process for $B<0.6$ T, as observed from the fits by taking into account the third term in Eq. (3). The temperature dependence of the coefficients of linear negative MR can be useful to identify the nature of the scattering process. The coefficient of the linear term (a_1), obtained from the fitting, is plotted as a function of temperature in a log-log scale [Fig. 3(c)]. For "strong scattering limit," a_1 is expected to be constant, while it increases with temperature in the "weak scattering limit."[25] The temperature dependence of a_1 points to the latter process in our network. The theoretical model[19] predicts T^{-s} behavior for a_1 and the exponent s is sensitive to the nature of disorder and dimensionality involved in the transport. The estimated values are $s=7/8$ for dimension $d=3$ and $s=1$ for $d=2$.[19]

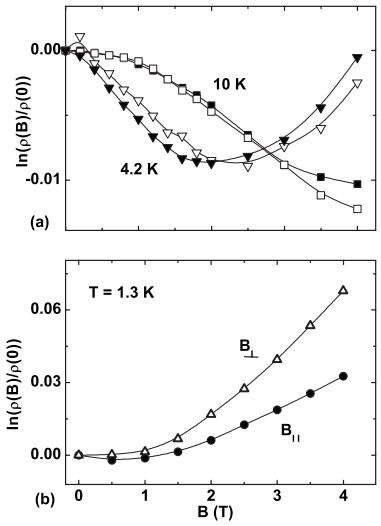

FIG. 4. (a) Field dependence of MR for transverse (open symbols) and longitudinal fields (filled symbols) at 4.2 K (triangles) and 10 K (squares). (b) Field dependence of MR for transverse (open symbols) and longitudinal fields (filled symbols) at 1.3 K. (Solid curves are a guide to the eye.)

The observed exponent for our network is $s=1.04\pm0.15$, a value that is close to 1. Since the exponents for both dimensions are close, an interpretation for dimensionality must rely on the anisotropy of MR. Furthermore, this model indicates that the numerical value of a_1 has some relation to the density of scattering sites, which in this context comprises the extent of defects, tube-tube intersections, volume packing fraction, etc. The physical relevance of a_2, in terms of localization length, is already described in Eq. (2).

A comparison of the MR for transverse and longitudinal fields is shown in Fig. 4. The forward interference mechanism, which is relevant at low fields, shows a weak anisotropy, as seen from the MR at 4.2 K [Fig. 4(a)]; at 10 K, the MR is nearly independent of the field direction. According to the forward interference models,[17–19] this is expected when the effective dimensionality is between 2 and 3, closer to the latter. These models rely on the concept of averaging the hops in a "cigar-shaped" area through which the magnetic flux penetrates. While moving from three to two dimensions, the hopping paths get increasingly confined to the plane of the sample, thereby hardly any area is present to the longitudinal magnetic field and this causes the anisotropy in negative MR. However, the anisotropy of wave-function shrinkage is much more pronounced, as seen from the MR at 1.3 K [Fig. 4(b)]. The difference in the extent of anisotropy further confirms that two different mechanisms are responsible for the observed MR, each being dominant at different temperature intervals.

In summary, we have presented low temperature magnetotransport measurements on transparent SWNT films. Interplay of two effects—a forward interference mechanism and wave-function shrinkage—are observed in a Coulomb gap variable-range hopping regime. The temperature dependence of low-field negative magnetoresistance, with exponent $s\sim1$, points to the network being in the weak scattering limit. The data analysis gives an estimate for both localization length and Coulomb gap. The behavior of magnetotransport indicates the extent of disorder and tube intersections in the nanotube network, both can serve as scattering centers for the electrons undergoing hops. A study of the scattering process from MR data in transparent SWNT networks is quite essential toward the understanding of transport in this form of SWNT. This particular data analysis consistently takes into account the various processes involved in the low temperature transport in these systems.

These measurements were performed at the DST National Facility for Low Temperature and High Magnetic Field, Bangalore (the authors thank V. Prasad). M.J. would like to thank CSIR, New Delhi, for financial assistance, and Y.-P.S. acknowledges financial support from the U.S. National Science Foundation.

*manu@physics.iisc.ernet.in

[1] S. N. Song *et al.*, Phys. Rev. Lett. **72**, 697 (1994).
[2] M. Baxendale *et al.*, Phys. Rev. B **56**, 2161 (1997).
[3] R. Tarkiainen *et al.*, Phys. Rev. B **69**, 033402 (2004).
[4] G. T. Kim *et al.*, Phys. Rev. B **58**, 16064 (1998).
[5] J. Vavro *et al.*, Phys. Rev. B **71**, 155410 (2005).
[6] D. P. Wang *et al.*, arXiv:cond-mat/0610747 (unpublished).
[7] G. Grüner, J. Mater. Chem. **16**, 3533 (2006).
[8] D. Hecht *et al.*, Appl. Phys. Lett. **89**, 133112 (2006).
[9] D. Zhang *et al.*, Nano Lett. **6**, 1880 (2006).
[10] H. Li *et al.*, J. Am. Chem. Soc. **126**, 1014 (2004).
[11] Y.-P. Sun, U.S. Patent Application No. 2006/0054555 A1 (pending).
[12] V. Skákalová *et al.*, Phys. Rev. B **74**, 085403 (2006).
[13] A. G. Zabrodskii, Philos. Mag. B **81**, 1131 (2001).
[14] A possible comparison of our unscreened network can be made with the nonoriented undoped pulsed laser vaporized SWNT (Vavro *et al.*, Ref. 5); the latter is a "bulk" sample showing 3D Mott VRH.
[15] J. M. Benoit *et al.*, Phys. Rev. B **65**, 241405(R) (2002).
[16] M. Reghu *et al.*, Phys. Rev. B **49**, 16162 (1994).
[17] V. L. Nguyen *et al.*, Sov. Phys. JETP **62**, 1021 (1985).
[18] M. E. Raikh and G. F. Wessels, Phys. Rev. B **47**, 15609 (1993).
[19] W. Schirmacher, Phys. Rev. B **41**, 2461 (1990).
[20] B. I. Shklovskii and A. L. Efros, *Electronic Properties of Doped Semiconductors* (Springer-Verlag, Berlin, 1984).
[21] This estimate for the gap assumes a 3D electronic system; this is justified by the nearly isotropic negative MR for parallel and perpendicular fields.
[22] B. Gao *et al.*, Phys. Rev. B **74**, 085410 (2006).
[23] R. Rosenbaum *et al.*, Phys. Rev. B **63**, 094426 (2001).
[24] M. Benzaquen *et al.*, Phys. Rev. B **38**, 10933 (1988).
[25] N. V. Agrinskaya and V. I. Kozub, Phys. Status Solidi B **205**, 11 (1998).